

## Open-Stopband Suppression and Cross-Polarization Reduction of a Substrate Integrated Waveguide Leaky-Wave Antenna

Debabrata K. Karmokar\*, Shu-Lin Chen, Pei-Yuan Qin, and Y. Jay Guo  
 Global Big Data Technologies Centre (GBDTC), Faculty of Engineering and Information Technology  
 University of Technology Sydney, Ultimo, NSW 2007, Australia

### Abstract

Most leaky-wave antennas (LWAs) suffer from significant gain degradation when the main beam points towards broadside. This is because an open stopband (OSB) restricts broadside radiation. In this paper, a method to suppress the OSB of a periodic substrate integrated waveguide (SIW) LWA is discussed. By simultaneously introducing a slot and a partially radiating wall in each unit cell the impedance in the OSB region has been matched and hence a continuous beam scan through broadside is achieved. The developed LWA can scan its main beam from  $-74^\circ$  continuously to  $+40^\circ$  when the frequency varies from 7.45 to 10.55 GHz, with a broadside gain and a level of cross-polarization for the broadside beam of 10.8 dB and  $-21.37$  dB, respectively.

### 1. Introduction

Some exceptional features have made leaky-wave antennas (LWAs) attractive, such as their low-profile configuration and more importantly inherent beam-scanning ability with frequency [1]-[6]. Inherent beam scanning can greatly reduce the complexity of a system. Moreover, LWAs can be integrated easily with circuits for applications in the microwave and millimeter-wave frequency ranges [7]. They can find a wide range of applications including radars, missiles, aircraft, etc. [8]-[10].

Although the main beam direction can be changed with frequency, for most uniform LWAs the scanning range is limited within the forward quadrant, i.e., a region between the near broadside and near endfire. They are also generally unable to scan the radiation beam through the broadside because of the restriction from an open stopband (OSB), and hence a gain degradation occurs [11], [12].

Several methods have been reported so far to suppress the OSB and realize a continuous beam scan. One popular method is designing an LWA using a composite right/left handed (CRLH) structure, and this type of antenna is called a CRLH LWA. A CRLH LWA can scan its beam through the broadside when a balanced condition (when  $L_R/L_L = C_R/C_L$ , where,  $L_R$ ,  $L_L$ ,  $C_R$ , and  $C_L$  are the right-handed (RH) inductance, left-handed (LH) inductance, RH capacitance, and LH capacitance, respectively) is achieved [13], [14]. Another method is to excite the  $n = -1$  spatial harmonic from a periodic structure [15], [16]. However, it is found that limited research is focused on continuous beam scan from a periodic structure compared to a CRLH structure.

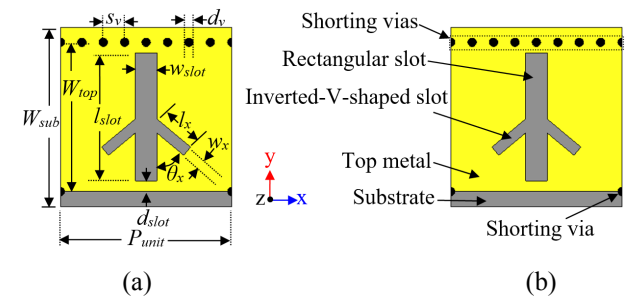


**Figure 1.** Top view of a unit cell with a rectangular and an inverted-V-shaped slot with partially radiating wall: (a) detailed dimensions and (b) name of different parts of the unit cell.

In this paper, a periodic LWA on a SIW is presented that realizes a continuous beam scan with low cross-polarization. It utilizes a rectangular slot on the top patch and simultaneously introduces a partially radiating via wall to suppress the open stopband. To reduce the cross-polarization level an additional inverted-V-shaped slot is etched on the patch.

In this paper, a periodic LWA on a SIW is presented that realizes a continuous beam scan with low cross-polarization. It utilizes a rectangular slot on the top patch and simultaneously introduces a partially radiating via wall to suppress the open stopband. To reduce the cross-polarization level an additional inverted-V-shaped slot is etched on the patch.

### 2. Suppression of Open Stopband

Fig. 1 shows the antenna unit cell, in which Fig. 1(a) represents the detailed dimensions, and the names of the different parts are highlighted in Fig. 1(b), designed on a Rogers RT5870 substrate. The parameters of the substrate are: dielectric constant ( $\epsilon_r$ ) = 2.33, loss tangent ( $\tan \delta$ ) = 0.0012, and thickness = 1.575 mm. It is seen that the unit cell consists of a rectangular transverse slot at the center of the top metal together with an inverted-V-shaped slot. A group of closely placed shorting vias (center-to-center distance of  $S_v$ ) connects the upper edge of the top metal to the ground plane. To enhance power leakage from the structure the vias in the lower wall are placed to maintain a large distance that is indeed equal to the length of the unit cell ( $P_{unit}$ ). By changing the distance between the lower edge vias the leakage can be controlled [17], [18].

**Table 1.** Dimensions of the unit cell and the antenna. All the dimensions are in mm except  $\theta_x$  which is in degree.

$P_{unit}$	$W_{sub}$	$W_{top}$	$l_{slot}$	$w_{slot}$	$l_x$	$w_x$	$d_v$
16	16.8	14	12	2	4.11	1	0.8
$s_v$	$d_{slot}$	$l_{f1}$	$l_{f2}$	$w_{f1}$	$w_{f2}$	$\theta_x$	$L_{Ant}$
2	1	4.5	7.75	4	8	$50^\circ$	249.5

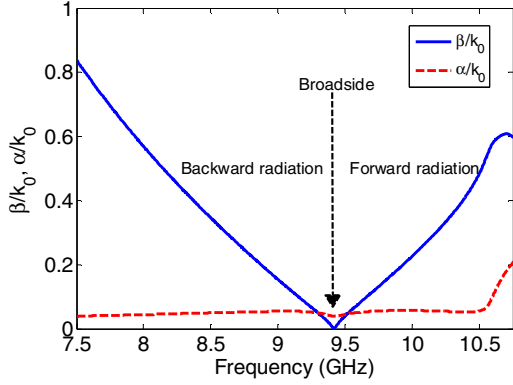


**Figure 2.** Dispersion diagrams for the unit cell in Fig. 1.

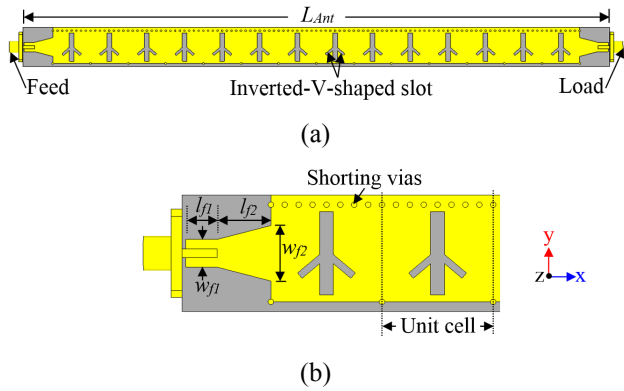


**Figure 3.** Configuration of the proposed SIW based LWA with a rectangular and an inverted-V-shaped slot in each unit cell: (a) top view of the complete antenna structure, and (b) a magnified section near the feed of the antenna with detailed dimensions of the feed line.

For a periodic LWA, a continuous backward to forward beam scan can be achieved by exciting the  $n = -1$  space harmonic, and the main beam direction of this radiation is given by [12], [16]

$$\theta_{n=-1}(f) \approx \sin^{-1} \left[ \frac{\beta_{n=-1}(f)}{k_0(f)} \right] \quad (1)$$

In (1),  $k_0$  is the free-space wavenumber, and  $\beta_{n=-1}$  is the phase constant which is given by

$$\beta_{n=-1} = \beta_0 - \frac{2\pi}{P_{unit}} \quad (2)$$

For a continuous beam scan through broadside, simultaneous fulfilment of two conditions is required.

These are: a linear variation of the phase constant (i.e., no bandgap), and the leakage from the structure should not change abruptly [12], [19]. To investigate the properties of the antenna, the dispersion diagram of the unit cell is obtained first, since from the dispersion diagram the characteristics of the antenna structure can be determined easily and effectively.

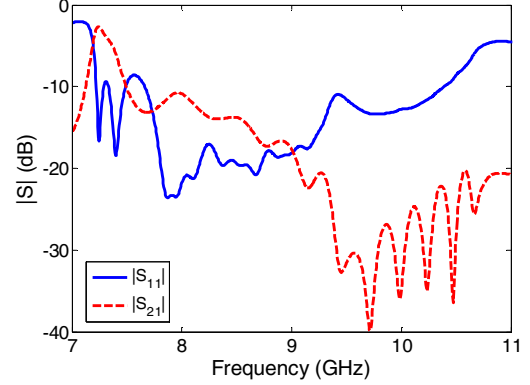


**Figure 4.** Simulated S-parameters of the LWA in Fig. 3.

Fig. 2 shows the dispersion diagram for the unit cell in Fig. 1 obtained from the S-parameters by simulating the unit using two ports, one at each side. As can be seen, there is a smooth transition between the forward and backward leaky regions, i.e. no bandgap. The normalized attenuation constant curve is also very flat without any null or bump. It is concluded that an LWA using this unit cell would enable a continuous beam scan through broadside without significant gain loss. The next section discusses the performance of a complete antenna made out using this unit cell.

### 3. Antenna Configuration

The configuration of the SIW LWA is presented in Fig. 3. A total of 14 unit cells are used in the antenna design. Fig. 3(a) shows the top view of the complete antenna structure, and a close view of the feed section is shown in Fig. 3(b). The antenna is fed by a tapered microstrip matching line from the left end, and another matching line with the same dimensions is located at the other end (right) as shown in Fig. 3(a) for terminating in a matched load to avoid unwanted reflected waves. The dimensions of the unit cell are already given in Table 1 and the dimensions of the matching tapered line together with the length ( $L_{Ant} = 7.83\lambda_0$  at 9.41 GHz) of the antenna in millimeters are also listed there.

### 4. Results and Discussion

The scattering parameters are shown in Fig. 4, obtained from a full-wave simulation of the antenna. The partial radiating wall and slot-loaded LWA has a  $-10$  dB reflection-coefficient bandwidth of 7.66 - 10.1 GHz. The reflection coefficient is higher than  $-10$  dB but remains below  $-8$  dB for frequencies up to 10.55 GHz, and below

−8.6 dB for frequencies down to 7.45 GHz. The  $|S_{21}|$  at 7.45 GHz is  $< -6.2$  dB and decreases with frequency, e.g. −18.87 dB at 9 GHz, indicating the good radiation performance of the antenna.

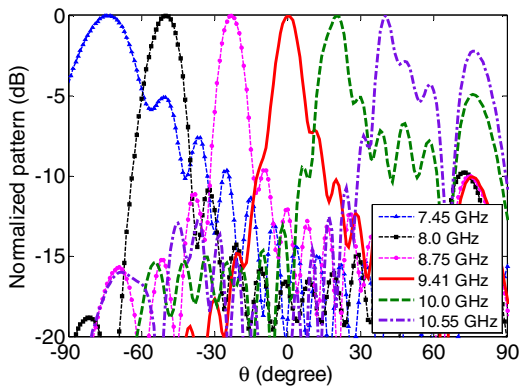


**Figure 5.** Simulated radiation patterns (normalized) of the LWA in Fig. 3.

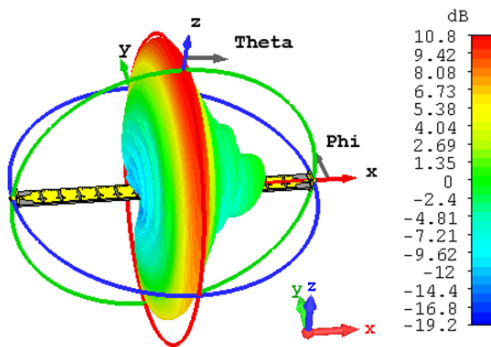


**Figure 6.** 3-D radiation (gain) pattern of the LWA in Fig. 3 when the main beam points at the broadside.

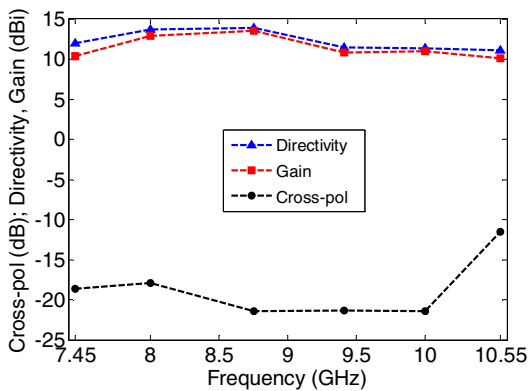


**Figure 7.** Simulated directivity, gain and cross-polarization level of the LWA in Fig. 3.

The simulated normalized radiation (gain) patterns of the antenna in Fig. 3 are shown in Fig. 5 to represent the continuous beam scanning performance of the antenna. Six beam directions are shown here for six different frequency points, from a lower value (7.45 GHz) to a higher value (10.55 GHz). As predicted from the

dispersion diagram the beam direction  $\theta$  is negative, i.e., the main beam points at the backward direction, at lower frequencies until the beam points at the broadside. Once the beam points at the broadside, with an increase of frequency the  $\theta$  values become positive, i.e., the beam scans in the forward direction. The beam direction ( $\theta$ ) for these six frequencies, i.e., 7.45, 8, 8.75, 9.41, 10, and 10.55 GHz, are  $-74^\circ$ ,  $-50^\circ$ ,  $-23^\circ$ ,  $0^\circ$ ,  $+20^\circ$ , and  $+40^\circ$ , respectively. A 3-D radiation pattern for the broadside beam is also presented in Fig. 6. As the antenna is 1-D it produces a fan-shaped beam in which the beam is wide in the y-z-plane and narrow in the x-z-plane. The shape of the radiating beam can be easily seen from Fig. 6.

Finally, the directivity and gain of the antenna for these six frequency points are shown in Fig. 7 together with the cross-polarization level as a function of frequency. The directivity of the antenna varies between 11.1 and 13.91 dBi within the frequency range between 7.45 and 10.55 GHz and the gain varies between 10.05 and 13.45 dBi. Note that leakages from slots and the partially radiating wall contribute to the far-field radiation, while the one from the partially radiating wall increases the cross-polarization. The inverted-V-shaped slot in each unit cell reduces the cross-polarization of the antenna, which varies between  $-21.48$  and  $-11.52$  dB within the beam scan range and is lower than 17.93 dB between 7.45 and 10 GHz.

## 5. Conclusion

This paper discusses a method to suppress the open stopband of an LWA is discussed here by etching a slot on the patch and making one of the SIW walls partially radiating. In this manner, the open stopband is suppressed completely. A full LWA was then designed, simulated and optimized. The final antenna can scan its main beam continuously from  $-74^\circ$  to  $+40^\circ$  with a gain of over 10 dBi when the source frequency varies from 7.45 to 10.55 GHz. Due to page limitations, inclusion of more results is not possible. Measured results will be presented in the conference as a further validation. Because of the structural simplicity this type of LWA can be a potential candidate for various beam-scanning applications.

## 6. Acknowledgements

This work was supported by the Australian Research Council (ARC) under a Discovery Project (DP) (Grant no. 160102219)

## 7. References

1. D. R. Jackson, C. Caloz, and T. Itoh, “Leaky-wave antennas,” *Proceedings of the IEEE*, **100**, 7, pp. 2194–2206, July 2012.
2. D. K. Karmokar, K. P. Esselle, and T. S. Bird, “Wideband Microstrip Leaky-Wave Antennas With Two

- Symmetrical Side Beams for Simultaneous Dual-Beam Scanning,” *IEEE Transactions on Antennas and Propagation*, **64**, 4, pp. 1262-1269, April 2016. doi: 10.1109/TAP.2016.2529646.
3. L. Chang, Z. Zhang, Y. Li, S. Wang, and Z. Feng, “Air-Filled Long Slot Leaky-Wave Antenna Based on Folded Half-Mode Waveguide Using Silicon Bulk Micromachining Technology for Millimeter-Wave Band,” *IEEE Transactions on Antennas and Propagation*, **65**, 7, pp. 3409-3418, July 2017. doi: 10.1109/TAP.2017.2700040.
4. D. K. Karmokar, Y. J. Guo, P.-Y. Qin, K. P. Esselle, and T. S. Bird, “Forward and Backward Beam-Scanning Tri-Band Leaky-Wave Antenna,” *IEEE Antennas and Wireless Propagation Letters*, **16**, pp. 1891-1894, 2017. doi: 10.1109/LAWP.2017.2685439.
5. Q. Lai, C. Fumeaux, and W. Hong, “Periodic leaky-wave antennas fed by a modified half-mode substrate integrated waveguide,” *IET Microwaves, Antennas & Propagation*, **6**, 5, pp. 594–601, April 2012. doi: 10.1049/iet-map.2011.0203.
6. K. Patra, S. Dhar, and B. Gupta, “Design guidelines for single and dual wide band leaky periodic microstrip line antennas,” *International Journal of RF and Microwave Computer Aided Engineering*, **28**, 6, e21288, August 2018, doi: 10.1002/mmce.21288.
7. D. K. Karmokar and K. P. Esselle, “Periodic U-Slot-Loaded Dual-Band Half-Width Microstrip Leaky-Wave Antennas for Forward and Backward Beam Scanning,” *IEEE Transactions on Antennas and Propagation*, **63**, 12, pp. 5372-5381, December 2015. doi: 10.1109/TAP.2015.2490252.
8. D. Xie, L. Zhu and X. Zhang, “An  $EH_0$  Mode Microstrip Leaky-Wave Antenna With Periodical Loading of Shorting Pins,” *IEEE Transactions on Antennas and Propagation*, **65**, 7, pp. 3419-3426, July 2017. doi: 10.1109/TAP.2017.2700882.
9. D. K. Karmokar and Y. J. Guo, “Planar leaky-wave antennas for low-cost radar,” *IEEE-APS Topical Conference on Antennas and Propagation in Wireless Communications (APWC)*, Verona, 2017, pp. 112-115. doi: 10.1109/APWC.2017.8062255.
10. D. K. Karmokar and Y. J. Guo, “Continuous Backward-to-Forward Beam-Scanning Conformal Leaky-Wave Antenna,” *IEEE 7<sup>th</sup> Asia-Pacific Conference on Antennas and Propagation*, New Zealand, 2018.
11. A. Sarkar *et al.*, “Composite right/left-handed based compact and high gain leaky-wave antenna using complementary spiral resonator on HMSIW for Ku band applications,” *IET Microwaves, Antennas & Propagation*, **12**, 8, pp. 1310-1315, 2018. doi: 10.1049/iet-map.2017.0478.
12. D. K. Karmokar, Y. J. Guo, P.-Y. Qin, S. Chen, and T. S. Bird, “Substrate Integrated Waveguide-Based Periodic Backward-to-Forward Scanning Leaky-Wave Antenna With Low Cross-Polarization,” *IEEE Transactions on Antennas and Propagation*, **66**, 8, pp. 3846-3856, August 2018. doi: 10.1109/TAP.2018.2835502.
13. M. R. M. Hashemi and T. Itoh, “Evolution of Composite Right/Left-Handed Leaky-Wave Antennas,” *Proceedings of the IEEE*, **99**, 10, pp. 1746–1754, October 2011. doi: 10.1109/JPROC.2011.2157797.
14. Nasimuddin, Z. N. Chen, and X. Qing, “Multilayered Composite Right/Left-Handed Leaky-Wave Antenna With Consistent Gain,” *IEEE Transactions on Antennas and Propagation*, **60**, 11, pp. 5056–5062, November 2012. doi: 10.1109/TAP.2012.2207680
15. Y. Lyu *et al.*, “Leaky-Wave Antennas Based on Noncutoff Substrate Integrated Waveguide Supporting Beam Scanning From Backward to Forward,” *IEEE Transactions on Antennas and Propagation*, **64**, 6, pp. 2155-2164, June 2016. doi: 10.1109/TAP.2016.2550054.
16. F. Xu, K. Wu, and X. Zhang, “Periodic Leaky-Wave Antenna for Millimeter Wave Applications Based on Substrate Integrated Waveguide,” *IEEE Transactions on Antennas and Propagation*, **58**, 2, pp. 340-347, February 2010. doi: 10.1109/TAP.2009.2026593.
17. A. J. Martinez-Ros, J. L. Gomez-Tornero, and G. Goussetis, “Planar Leaky-Wave Antenna With Flexible Control of the Complex Propagation Constant,” *IEEE Transactions on Antennas and Propagation*, **60**, 3, pp. 1625-1630, March 2012. doi: 10.1109/TAP.2011.2180320.
18. Feng Xu and Ke Wu, “Guided-Wave and Leakage Characteristics of Substrate Integrated Waveguide,” *IEEE Transactions on Microwave Theory and Techniques*, **53**, 1, pp. 66-73, January 2005. doi: 10.1109/TMTT.2004.839303.
19. A. A. Oliner and D. R. Jackson, “Leaky-wave antennas,” in *Antenna Engineering Handbook*, J. L. Volakis, Ed., NY, USA: McGraw-Hill, 2007, ch. 11.